

# 1D Borophosphates for Use as Electrolyte Membranes in Solid Acid Fuel Cells

J. August Ridenour<sup>1</sup>, Brian L. Chaloux<sup>1</sup>, Michelle D. Johannes<sup>2</sup>, Matthew T. Finn<sup>1</sup>,  
Heonjune Ryou<sup>2</sup>, Albert Epshteyn<sup>1</sup>

<sup>1</sup> Chemistry Division, <sup>2</sup> Materials Science and Technology Division  
US Naval Research Laboratory  
4555 Overlook Ave, SW, Washington, DC 20375  
brian.chaloux@nrl.navy.mil

## Abstract

We investigate the proton conduction, thermal stability, and viability of the borophosphate compounds sodium borophosphate (NaBOB, Na<sub>5</sub>[BOB(PO<sub>4</sub>)<sub>3</sub>]) and ammonium borophosphate (NH<sub>4</sub>BOB, (NH<sub>4</sub>)<sub>3</sub>H<sub>2</sub>[BOB(PO<sub>4</sub>)<sub>3</sub>]) for use as solid polyelectrolytes in intermediate temperature solid acid fuel cells. Bulk synthesis methods are presented for laboratory scale (> 5 g) batch preparation of each borophosphate. Electrochemical impedance spectroscopy (EIS) was utilized to determine the ionic conductivities of NH<sub>4</sub>BOB and NaBOB as a function of temperature; conductivities under dry N<sub>2</sub> flow reach 2 μS cm<sup>-1</sup> and 0.9 μS cm<sup>-1</sup> at 200 °C, respectively. Although NH<sub>4</sub>BOB displays higher ionic conductivity, thermal gravimetric analyses (TGA) show much higher thermal stability in NaBOB, which remains unperturbed to 600+ °C. The thermal stability of NaBOB was also assessed under reducing atmosphere (1 atm H<sub>2</sub>), exhibiting no reductive mass loss up to at least 400 °C. *Ab initio* molecular dynamics (MD) simulations help elucidate the mechanism of ionic conduction in these borophosphates, showing that free H<sup>+</sup> mobility is coupled to the gyrational mobility of the polyanionic borophosphate chains.

## Keywords

borophosphate; proton conductor; fuel cell

## Introduction

Over the past few decades, solid acid fuel cells (SAFCs) have been investigated as alternatives to polymer exchange membrane (PEMFCs) and solid oxide (SOFCs) fuel cells with the promise of enabling fuel cell device operation at ‘intermediate’ temperatures.<sup>1-3</sup> Operating at intermediate temperatures – between 100 and 450 °C – allows for improved water management, heat rejection, and catalytic activity, yet avoids the expensive high-temperature refractory materials required in SOFCs.<sup>1, 4, 5</sup> At these temperatures, polymer-electrolyte membrane (PEM) electrolytes that require water for proton conduction, dry out and can no longer be used. Also, SOFC ceramic oxide electrolytes are not able to operate in this relatively low temperature regime since they rely on high temperature mobility of the oxide anion, which has a high activation energy for motion. Achieving high efficiency fuel cell

operation at intermediate temperatures thus necessitates the development of *proton* conducting solid materials sufficient thermal stability that are compatible with hydrogen under operating conditions.

Solid acids are a subset of protic, crystalline materials, such as CsHSO<sub>4</sub> and CsH<sub>2</sub>PO<sub>4</sub>, that bear labile protons in the solid state. The aforementioned CsHSO<sub>4</sub> and CsH<sub>2</sub>PO<sub>4</sub> have been investigated as solid polyelectrolytes in SAFCs for over 20 years.<sup>6-8</sup> These solids exhibit a ‘superprotonic’ phase transition at elevated temperature wherein the protic anion becomes rotationally disordered, causing a solid-solid transition to a new phase that exhibits several orders of magnitude increase in proton mobility.<sup>9</sup> Of these materials, CsH<sub>2</sub>PO<sub>4</sub> (cesium dihydrogen phosphate, CDP) has emerged as a primary contender for SAFCs due to its high proton conductivity above 225 °C and its good stability in a reducing environment,<sup>8, 10, 11</sup> however, CDP is thermodynamically unstable above this superprotonic transition, slowly dehydrating to inert pyro- and polyphosphates unless hydrated with a constant flow of humidified ( $p_{H_2O} \sim 0.3$  atm) gas.<sup>8</sup>

To circumvent material shortfalls and push the upper operating temperature limit of solid acid membrane materials, we continue to investigate a broad class of solid acid compounds characterized by one-dimensional (1D) polyanionic chains. Borosulfates – chemical formula X[B(SO<sub>4</sub>)<sub>2</sub>] – are 1D polyanions containing alternating SO<sub>4</sub> and BO<sub>4</sub> tetrahedra with interstitial cations (X = NH<sub>4</sub>, K, etc.). In general, these materials are thermally stable above 250 °C even without humidification, allowing the elimination of cumbersome humidification systems.<sup>4, 12</sup> Herein, we discuss a related class of 1D solid acids that substitute sulfate with the more thermally and reductively robust phosphate anion: borophosphates. The ammonium and sodium borophosphate variants (NH<sub>4</sub>BOB and NaBOB, respectively) are investigated as potential solid polyelectrolyte membrane materials by analyzing their ionic conductivity, as well as thermal and chemical stability. *Ab initio* molecular dynamics (MD) computational simulations illustrate the functional similarity of borosulfates and borophosphates<sup>4, 12</sup>: that temperature dependent gyrational mobility of the 1D chains facilitates proton hopping, with both material types exhibiting quite high proton mobility.

## Experimental

Ammonium- and sodium-bearing borophosphates were synthesized in a low temperature flux reaction using ionic liquids (e.g., 1-butyl-3-methylimidazolium bromide, BMIM-Br) in a Teflon-lined stainless steel autoclave by heating the reactants without active mixing at 100–250 °C for 1–7 days. The solid white products were washed sequentially with glacial acetic acid, isopropanol, and diethyl ether to remove residual ionic liquid and unreacted starting materials.

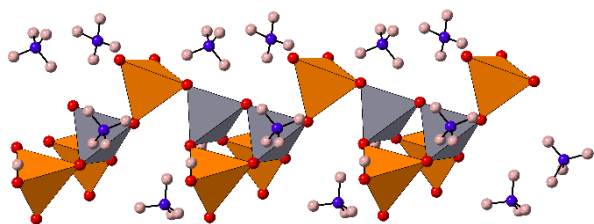


**Figure 1.** Structure of  $\text{NH}_4\text{BOB}$ . Orange and grey polyhedra represent  $\text{PO}_4$  and  $\text{BO}_4$  units, while red, blue, and white spheres represent oxygen, nitrogen, and hydrogen atoms, respectively.  $\text{NaBOB}$  exhibits the same polyanion structure.

Single crystal X-ray diffraction was utilized to determine the novel crystal structure of  $\text{NH}_4\text{BOB}$ ,  $(\text{NH}_4)_3[\text{BOB}(\text{PO}_4)(\text{PO}_3\text{OH})_2]$ , using a MiTeGen MicroMount™ and reflections collected with  $0.5^\circ$  scans on a Bruker D8 Quest diffractometer equipped with a Photon II detector using  $\text{Mo K}\alpha$  ( $\lambda = 0.71073 \text{ \AA}$ ) radiation at 100(2) K. The data were integrated, absorption corrected, solved (intrinsic phasing), and refined with SAINT, SADABS, ShelXT, and SHELX2018-1, respectively, all within the APEX III software suite.<sup>13–17</sup> The crystal structure was illustrated (**Figure 1**) with CrystalMaker.<sup>18</sup> Thermal stabilities were assessed using thermogravimetric analysis (TGA, Netzch Jupiter system) at a  $10 \text{ K min}^{-1}$  scan rate under an argon atmosphere. A custom gas pressure thermogravimetric analysis instrument was used to investigate thermal decomposition under reducing conditions (800 torr  $\text{H}_2$ ) and results were compared to decomposition under inert atmosphere for a qualitative assessment of reductive chemical stability.

Disc-shaped pellets (100–200 mg, 300–700  $\mu\text{m}$  thick) were pressed in a 12.7 mm tungsten carbide die between Carver press platens ( $\approx 240 \text{ MPa}$ , 200 °C for 16 h) for electrochemical impedance spectroscopy (EIS) analysis of ionic conductivity. Bulk density of the pellets was determined using a digital micrometer to measure thickness and an analytical balance for mass. Scanning electron microscopy (SEM) was performed on a Quattro environmental SEM at 20 kV to acquire images of  $\text{NaBOB}$  post-consolidation to qualitatively assess the degree of consolidation and porosity of the pellet. Ionic conductivity was determined by performing EIS on pellets sandwiched between gold-coated (50 nm by sputtering), porous, powder-sintered steel electrodes using a Gamry Reference 3000 potentiostat applying 100 mV AC over a frequency range of

1 MHz to 1 Hz. The sample-electrode assembly was mounted in a machined aluminum cell allowing for precise heating ( $\pm 0.1 \text{ }^\circ\text{C}$ ) with cartridge heaters and dry nitrogen to be flowed over both sides of the sample. Raw impedance spectra were fit with a modified Randles circuit and conductivities were estimated from the calculated electrolyte resistance and measured dimensions of each sample.

To assess proton diffusivity, we used ab-initio molecular dynamics (AIMD) to model the dynamics of  $2 \times 2 \times 2$  supercells of  $\text{NH}_4\text{BOB}$  and  $\text{NaBOB}$  (containing 32 total  $[\text{BOB}(\text{PO}_4)_3]^{5-}$  repeat units) with 1–4 excess  $\text{H}^+$  per supercell (charge balanced with a uniform negative background). Each cell at each proton concentration was fully relaxed at  $T=0$ , with a very high energy cutoff of 670 eV to ensure accurate stresses for lattice relaxation. An NRL-developed AIMD formulation<sup>19</sup> was used to simulate the cells at 900K over 16 ps with a 0.5 fs time step; input forces and energies were imported from the Vienna Ab Initio Simulation Program (VASP)<sup>20</sup> using the Perdew Burke Ernzerhof (PBE) approximation to the exchange correlation functional.<sup>21</sup>

## Discussion

The ‘BOB’ borophosphates are so named because of their characteristic bridging boron–oxygen–boron linkages along the backbone of the 1D polyanions. There exist three known BOBs, which are isostructural (but not isomorphous) in that the chemical composition and connectivity of the chain are identical, and only the charge balancing cations ( $\text{NH}_4^+$ ,  $\text{Na}^+$ , and  $\text{Rb}^+$ ) and unit cell vary.<sup>22, 23</sup> The  $\text{NH}_4^+$  variant ( $(\text{NH}_4)_3\text{H}_2[\text{BOB}(\text{PO}_4)_3]$ ,  $\text{NH}_4\text{BOB}$ ) is a novel compound (**Figure 1**) that can be synthesized in high isolated yield (70–90%) in the same manner as the  $\text{Na}^+$  and  $\text{Rb}^+$  variants using a novel process involving a low-temperature ionic liquid reaction, instead of the high temperature, molten-salt fluxes reported in prior literature.<sup>22, 23</sup> Under inert atmosphere,  $\text{NH}_4\text{BOB}$  and  $\text{NaBOB}$  are thermally stable up to 250 °C and 600 °C, respectively. In a reducing environment (800 mmHg  $\text{H}_2$ ), as would be experienced in an operating fuel cell,

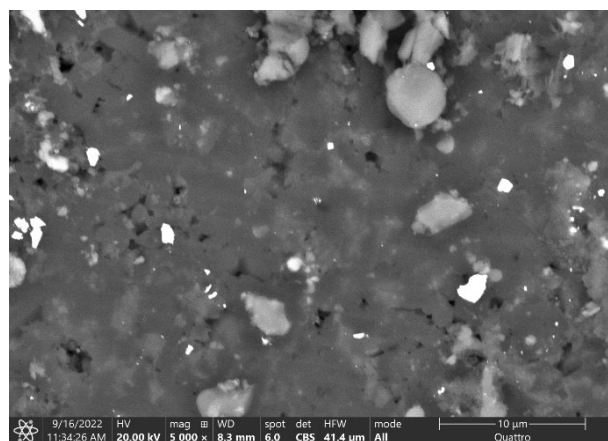


**Figure 2.** SEM image of a consolidated pellet of  $\text{NaBOB}$  showing sintering of grains.

NH<sub>4</sub>BOB loses significant mass below 200 °C, possibly through condensation and loss of H<sub>2</sub>O. In NaBOB, which lacks intrinsic protons, negligible thermal decomposition was observed under H<sub>2</sub> up to at least 450 °C.

Disc-shaped monolithic pellets were made by pressing small amounts of NH<sub>4</sub>BOB / NaBOB powder in a 12.7 mm diameter tungsten carbide die press while heating to 100 °C. On average, consolidation of the pellets was >90 % comparing volumetric pellet density to the density of a single crystal. SEM imaging (**Figure 2**) shows the deformation of individual crystallites in a NaBOB pellet and minimal retained porosity. To determine ionic conductivity, EIS was conducted on pellets after heating under flowing, dry N<sub>2</sub> to give approximately anhydrous conditions. Overall, NH<sub>4</sub>BOB exhibits slightly (~2x) higher ionic conductivity than NaBOB across the range of temperatures investigated (**Figure 3**), which may be due to the presence of intrinsic protic sites on the NH<sub>4</sub>BOB backbone. Although the performance of NaBOB is slightly lower than NH<sub>4</sub>BOB at comparable temperatures, its higher thermal stability allows for greater operational temperatures. The ionic conductivity of NH<sub>4</sub>BOB at 205 °C was measured to be 2.2 μS cm<sup>-1</sup>, whereas conductivity of NaBOB at 310 °C reached 7.5 μS cm<sup>-1</sup>.

Since these borophosphates are 1D chains, their mechanism of proton conduction is fundamentally dissimilar to the ‘superprotonic’ mobility observed in 0D solid acid electrolytes materials such as CDP. In separate studies on borosulfates,<sup>4, 12</sup> temperature dependent gyrational mobility of the chains was shown to allow efficient proton hopping pathways along and between chains as the sulfate oxygens move closer together. Molecular dynamics simulations of single crystal derived structural data for NH<sub>4</sub>BOB and NaBOB show a similar mechanism for 1D borophosphates; AIMD at 900K shows phosphate gyrational mobility facilitating the movement of extrinsic protons throughout the bulk of these materials.

## Conclusion

A class of one-dimensional borophosphates has been shown to be thermally and chemically stable under conditions relevant to intermediate temperature solid acid fuel cells (SAFC). These compounds, particularly sodium borophosphate (NaBOB), represent a group of 1D

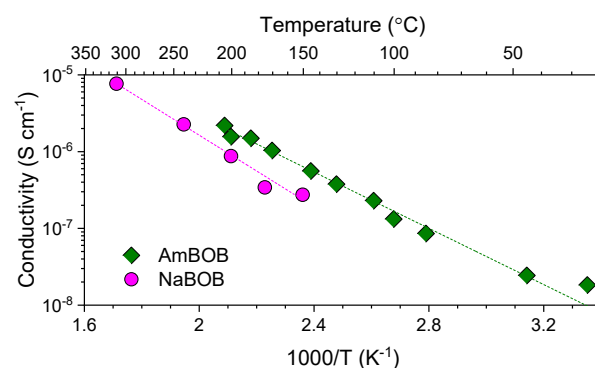


**Figure 3.** Temperature-dependent ionic conductivity of NH<sub>4</sub>BOB (green diamonds) and NaBOB (magenta circles) under dry N<sub>2</sub>.

polyelectrolytes having ionic conductivity and thermal properties well-suited for advanced SAFC technologies.

Modest ionic conductivities (2–8 μS cm<sup>-1</sup>) at elevated temperatures are driven by gyrational motion of the 1D chains, as highlighted by ab initio molecular dynamics simulations, lowering the energy barrier for proton hopping along and between chains. This provides high mobility to the existing free protons in the system, while the relatively low observed conductivities are driven by a lack to carriers and therefore low carrier concentrations. Efforts are currently underway to investigate these materials in hydrogen fuel cell systems as well as to modify the electrolyte by cation doping to improve proton conductivity and pellet consolidation.

## Acknowledgements

This material is based upon work supported by the Office of Naval Research through the U.S. Naval Research Laboratory. Dr. J. August Ridenour thanks the National Research Council for administering his postdoctoral fellowship.

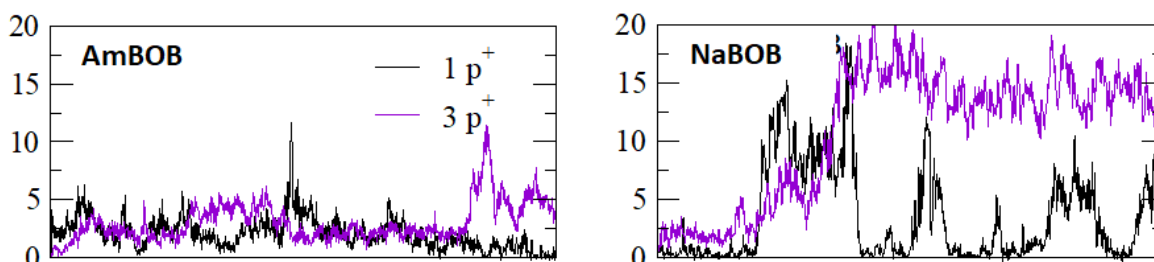


**Figure 4.** Average mean squared displacements (in Å<sup>2</sup>) of excess H<sup>+</sup> in NH<sub>4</sub>BOB (left) and NaBOB (right) tracked over 16 ps at 900K with 1 (black trace) or 3 (blue trace) H<sup>+</sup> per 2×2×2 supercell.

## References

1. Mohammad, N.; Mohamad, A. B.; Kadhum, A. A. H.; Loh, K. S., *Journal of Power Sources* **2016**, *322*, 77-92.
2. Ndubuisi, A.; Abouali, S.; Singh, L.; Thangadurai, C., *J. Mater. Chem. A* **2021**, *10*, 2196-2227.
3. Parekh, A., *Front. Energy Res.* **2022**, *10*, 956132.
4. Ward, M. D.; Chaloux, B. L.; Johannes, M. D.; Epshteyn, A., *Adv. Mater.* **2020**, *32* (42), 2003667.
5. Murthi, V. S.; Urian, C.; Mukerjee, S., *J. Phys. Chem. B* **2004**, *108* (30), 11011-11023.
6. Haile, S. M., *Nature* **2001**, *410*, 910-913.
7. Haile, S. M., *Materials Today* **2003**, *6* (3), 24-29.
8. Boysen, D. A.; Uda, T.; Chisholm, C. R. I.; Haile, S. M., *Science* **2004**, *303*, 68-70.
9. Chisholm, C. R. I.; Merle, R. B.; Boysen, D. A.; Haile, S. M., *Chem. Mater.* **2002**, *14* (9), 3889-3893.
10. Haile, S. M.; Chisholm, C. R. I.; Sasaki, K.; Boysen, D. A.; Uda, T., *Faraday Discussions* **2007**, *134*, 17-34.
11. Chisholm, C. R. I.; Haile, S. M., *Chem. Mater.* **2007**, *19* (2), 270-279.
12. Chaloux, B. L.; Ridenour, J. A.; Johannes, M. D.; Epshteyn, A., *Advanced Energy and Sustainability Research* **2022**, *3* (8).
13. SAINT, B. A. I. M., Wisconsin, USA, **2013**.
14. APEX III, B. A. I. M., Wisconsin, USA, **2013**.
15. Sheldrick, G. M., *Acta Crystallogr.* **2008**, *A64*, 112-122.
16. Sheldrick, G. M., *Acta Crystallogr.* **2015**, *C71* (1), 3-8.
17. Krause, L.; Herbst-Irmer, R.; Sheldrick, G. M.; Stalke, D., *J. Appl. Crystallogr.* **2015**, *48* (1), 3-10.
18. *CrystalMaker®: a crystal and molecular structure program for Mac and Windows*, CrystalMaker Software, Ltd: Oxford, England.
19. Perdew, J. P.; Burke, K.; Ernzerhof, M., *Phys. Rev. Lett.* **1996**, *77* (18), 3865-3868.
20. Bernstein, N.; Johannes, M. D.; Hoang, K., *Phys. Rev. Lett.* **2012**, *109* (20).
21. Kresse, G.; Hafner, J., *Phys. Rev. B* **1993**, *47* (1), 558-561.
22. Ewald, B.; Prots, Y.; Menezes, P.; Natarajan, S.; Zhang, H.; Knier, R., *Inorg. Chem.* **2005**, *44* (18), 6431-6438.
23. Hauf, C.; Friedrich, T.; Knier, R., *Z. Kristallogr.* **1995**, *210*, 446.